SCIENTIFIC REPORTS

Exploring the Reusability of Synthetically Contaminated Wastewater Containing Crystal Violet Dye using *Tectona grandis* Sawdust as a Very Low-Cost Adsorbent

Fouzia Mashkoor[1], Abu Nasar[1], Inamuddin[2,3] & Abdullah M. Asiri [2,3]

Present investigation explores the possible reusability of synthetically contaminated wastewater containing crystal violet (CV) organic dye using *Tectona grandis* sawdust (TGSD) waste as a very low-cost adsorbent. The adsorbent was characterized by proximate, SEM/EDX, FTIR, and XRD analyses. Batch adsorption studies were carried under changing conditions of contact time, the initial concentration of CV, pH, TGSD dose, TGSD particle size, and temperature. The experimental data were tested using Langmuir, Freundlich and Temkin isotherm models, and the data were best followed by Langmuir one. The kinetic results were examined in the light of different models and pseudo-second-order was obtained to be best obeyed. The values of $\Delta H°$ (28.642 kJ/mol), $\Delta G°$ (-10.776 to -7.080 kJ/mol) and $\Delta S°$ (121.8 J/K/mol) in the temperature range of 293–323 K suggested the overall process to be spontaneous, endothermic and associated with an increase in randomness. On the basis of experimental results and their analyses, it has been established that TGSD is one of the most effective adsorbents among those obtained from the domestic, agricultural and industrial wastes. Thus this adsorbent can be effectively utilized to make the impure wastewater reusable.

Safe and clean water is essential for human health and pleasure, ecosystems and also for a booming economy[1]. Deterioration of water quality and continuous decrease in the availability of fresh water are the matters of great concerns. The presence of contaminants like heavy metals, dyes, pesticides etc. steadily degrades the quality of water and is the major reason for several diseases and damage to human health[2–6]. Among the several pollutants, dyes are the only ones which can be visible to the naked eye even at very low concentration. Depending on their nature, concentration and exposure time the effects of dyes can be acute or chronic. Dyes can cause problems such as skin irritation, respiratory diseases, mental disorder, vomiting and in many cases they may be carcinogenic and mutagenic[7–9]. Dyes are used in a number of industries like rubbers, plastics, cosmetics, textile, food, leather, pharmaceutical, wood preserving chemicals, photographic, pulp and paper, petroleum industries etc.[10–12]. There is a long list of dyes available in the market with approximately 7×10^5 tonnes of annual production[13]. Crystal violet (CV) is a triarylmethane synthetic dye with deep purple hue. It has uses in paint and printing ink, veterinary medicines, etc. It also has antibacterial and antifungal properties. However, this dye has been reported to be toxic in several aspects and stays in the environment for a very long time[14]. Most of the dyes have high thermal and photostability and hard to decolourize due to their stable structure, non-biodegradability and synthetic origin[15,16]. Untreated or poorly treated effluents discharged from these industries are the reason for a serious threat to flora

[1]Department of Applied Chemistry, Faculty of Engineering and Technology, Aligarh Muslim University, Aligarh, 202002, India. [2]Chemistry Department, Faculty of Science, King Abdulaziz University, Jeddah, 21589, Saudi Arabia. [3]Centre of Excellence for Advanced Materials Research, King Abdulaziz University, Jeddah, 21589, Saudi Arabia. Correspondence and requests for materials should be addressed to A.N. (email: abunasaramu@gmail.com) or I. (email: inamuddin@rediffmail.com) or A.M.A. (email: aasiri2@kau.edu.sa)

and fauna[17]. One of the serious environmental concerns related to dyes is that it decreases the penetration of light radiation into the water which has disparaging effects on the photosynthetic activity of aquatic life and causes a deficiency of oxygen[18,19].

Thus, the removal of contaminants is essential to make the wastewater reusable. Different types of techniques have been developed for the treatment of water contaminants such as dyes, heavy metals, pesticides, fertilizers etc. to eliminate or reduce their hazardous impacts on the human and other living bodies. These include electro-dialysis[20], photocatalysis[21,22], nanofiltration membranes[23,24], electroflotation[25], electrokinetic/electrooxidation[26], coagulation-flocculation[12,27–29], reverse osmosis[30], ozonation[31,32], colloidal manganese dioxide oxidation[4,33–36], ion-exchange[19,37], anaerobic-aerobic[38], adsorption[39–42]. Out of these methods, adsorption has been observed to be most attractive one because this method is easy, effective, eco-friendly, and economical for the decontamination of dye-loaded effluents[43,44]. However, the choice of suitable adsorbent was always a challenging task. The conventional adsorbents like activated carbon and silica gel should be a primary choice but their usage is narrowed due to high cost and regeneration problems. In this context the adsorbents made from natural materials, agricultural, domestic and industrial wastes (e.g. tea waste[45], oil palm biomass[46], bagasse[47], citrus limetta[48], cucumis sativus[49], prosopis cineraria[50], Fe(III)/Cr(III) hydroxide[51], titania-silica[52], zeolite[53,54], cupuassu shell[55], chitosan[56–58] etc.) offer suitable alternatives for the adsorptive treatment of dyes from wastewater.

Teak (*Tectona grandis* Linn. f.) has the extraordinary weather resistant capacity and therefore found a place as one of the most popular hardwood timber species. *Tectona grandis* is native to tropical and subtropical countries[59,60]. The sawdust of teak tree is a waste product which can be gainfully utilized as a cheap adsorbent for the elimination of dyes from the aqueous solution. The present investigation has been planned with a prime objective to find out the suitability of *Tectona grandis* sawdust (TGSD) as an adsorbent for the removal of CV from laboratory synthesized wastewater. It has also been planned to conduct the experiments on variable experimental conditions such as adsorbent dose, dye concentration, pH of the medium, adsorbate-adsorbent contact time, the particle size of adsorbent and temperature because these factors play a significant role in the optimization of the process for better feasibility.

Materials and Methods

Materials. CV dye of the biological stain grade, obtained from Fisher Scientific, India was used as received without further purification. The following analytical reagent grade chemicals and reagents were used in the present investigation: HCl (Fisher Scientific, India), CH_3COOH (SD fine, India), NaOH (Merck, Germany) and KNO_3 (CDH, India). The stock solution of CV (1000 mg/L) was made by dissolving an appropriate amount of CV in the doubly distilled deionized water (DDDW).

Preparation and characterization of TGSD adsorbent. TGSD obtained from sawmill was cleaned comprehensively by DDDW to eliminate the dust, dirt and other surface contaminants. The washed mass was dried in sunlight under the cover of the white cotton sheet (making air gap of at least 4 cm between mass and sheet) for about 2 days and then in an oven at about 95 °C for 24 h. The dried material was crushed into the powder by a motor operated grinder and then screened through a standard sieve of 80 BSS mesh and then finally washed thoroughly with DDDW. The sieved powder (80 BSS mesh) was again dried in the oven at 105 °C for about 4 h. Thereafter the crude material mass was powderize in agate mortar pestle and separated through a set of sieves (80–150, 150–200 and >200 BSS scales) and the adsorbents of different size fractions were kept in airtight vessels.

The various components present in the TGSD adsorbent were determined by performing the proximate analysis. The Moisture content of TGSD sample was obtained by the official method of chemical analysis[61]. 2.0 g of the sample taken in a porcelain crucible was oven dried at 100 °C for 4 h. From the initial and final weight (W) of the filled and empty crucible the moisture content was calculated by using the following equation:

$$\% \text{ moisture content} = \frac{W_{initial,filled} - W_{final,filled}}{W_{initial,filled} - W_{final,empty}} \times 100 \tag{1}$$

The total ash content of the sample, based on the vaporization of water and volatile matters along with the burning of organic substances in presence of atmospheric oxygen, was measured by incinerating 2.0 g TGSD in porcelain crucible in a muffle furnace at 700 °C for 7 h. The % ash was calculated by using the following equation:

$$\% \text{ ash} = \frac{W_{ash}}{W_{TGSD}} \times 100 \tag{2}$$

The content of volatile matter was determined from the weights of 2.0 g of dry sample (W_{dry}) and heated sample (W_{heated}) at 550 °C (10 min) by using the following equation:

$$\% \text{ volatile matter} = \frac{W_{dry} - W_{heated}}{W_{dry}} \times 100 \tag{3}$$

The percent fixed carbon was evaluated by using the following equation:

$$\% \text{ fixed carbon} = 100 - \%(\text{moisture} + \text{ash} + \text{volatile matter}) \tag{4}$$

The morphological features of the CV unloaded and loaded TGSD were analyzed by using SEM/EDX (JEOL, JSM6510LV, Japan). FTIR spectrum of the TGSD was measured in the spectral range of 4000–400 cm^{-1} in the solid state. The adsorbent was also characterized by measuring the point of zero charge by employing the solid

addition method. XRD patterns of TGSD and CV adsorbed TGSD were recorded using X-ray diffractometer (Miniflex II, Rigaku, Japan) with CuKa radiation at the scanning speed of 10°/min with 2θ angle varying in the range of 5–60°.

Batch equilibrium studies. Batch experiments were conducted at the variable dose of TGSD, solution pH, initial concentrations of CV, the particle size of TGSD, adsorbate-adsorbent contact time and temperature. The time-dependent (3 to 180 min) measurements were conducted by adding 0.05 g of TGSD adsorbent into 25 ml of CV solution with varying initial concentration (25–150 mg/L) at room temperature. After filtering the adsorbent agitated adsorbate solution, the residual concentration of dye in the filtrate was determined by UV-VIS spectro-photometer at a pre-optimised λ_{max} (wavelength corresponding to maximum absorption) of 575 nm. The extent of dye adsorption, which is usually expressed by two parameters adsorption capacity (q) and percent removal efficiency (%R), and can be obtained by employing the following equations:

$$q_e = (C_o - C_e) \times \frac{V}{m} \tag{5}$$

$$\%R = \frac{(C_0 - C_t)}{C_0} \times 100 \tag{6}$$

where C is a concentration of CV (mg/L), V is the solution volume (L), m is the adsorbent mass (g). The subscript o, e and t represent the terms initial, equilibrium and anytime, respectively and will be used as and when required. The adsorption capacity at any time (q_t) can be computed by using analogous equation obtained by replacing the term C_e by C_t in equation (5).

Adsorption isotherm. The adsorption isotherm plays a major role in the strategy of any adsorbate-adsorbent system. It gives important information on adsorption mechanism, surface properties of adsorbent, the surface affinity of adsorbate onto the absorbent. The results of the present studies have been analyzed in three commonly used isotherm models as pronounced by their inventors, namely, Langmuir[62], Freundlich[62,63] and Temkin[64]. The linear mathematical forms are given below in respective order:

$$\frac{1}{q_e} = \frac{1}{q_m K_L C_e} + \frac{1}{q_m} \tag{7}$$

$$\ln q_e = \frac{1}{n}\ln C_e + \ln K_F \tag{8}$$

$$q_e = B \ln C_e + B \ln K_T \tag{9}$$

In the above equations, q_e is adsorption capacity at equilibrium, q_m (mg/g) is the theoretical Langmuir maximum adsorption capacity, K_L (L/mg) is the Langmuir adsorption constant, K_F ($mg^{1-1/n}L^{1/n}/g$) and n are the Freundlich constants, B (=RT/b), b (J/mol) and K_T (L/g) are the Temkin isotherm constants, T is the absolute temperature (K) and R is the universal gas constant (8.314 J/K/mol). Further, the important features of Langmuir isotherm may be expressed by a dimensionless quantity $R_L \left(= \frac{1}{1 + K_L C_o} \right)$, the value of which indicates the adsorption to be favourable (0–1), unfavourable (>1), linear (1) or irreversible (0).

Adsorption kinetics. The kinetics behind the removal of CV onto the surface of TGSD was studied by monitoring the experiments as a function of time. The experimental procedure was same as performed with the batch equilibrium studies. The adsorption results were analyzed in the light of three most commonly used kinetic models namely, pseudo-first order[65,66], pseudo-second order[67] and intraparticle diffusion[68,69]. The linear forms of these models in the respective order may be represented as:

$$\ln(q_e - q_t) = \ln q_e - K_1 t \tag{10}$$

$$\frac{t}{q_t} = \frac{1}{K_2 \, q_e^2} + \frac{t}{q_e} \tag{11}$$

$$q_t = K_{id} \, t^{1/2} + C \tag{12}$$

where K_1(1/min), K_2 (g/min mg), and K_{id} (mg min$^{-\frac{1}{2}}$/g) is the first-order rate constant, second-order rate constant, and intraparticle diffusion rate constant, respectively. The values of various kinetic parameters were determined from the respective linear plots (Section 3).

Adsorption thermodynamics. Thermodynamic factors, viz., Gibb's free energy (ΔG°), enthalpy (ΔH°), and entropy (ΔS°) change associated with adsorptive decontamination of CV by TGSD were calculated via the following equations:

$$\Delta G^\circ = -RT \ln K_c \tag{13}$$

$$\ln K_c = \frac{-\Delta G^\circ}{RT} = \frac{-\Delta H^\circ}{RT} + \frac{\Delta S^\circ}{R} \tag{14}$$

where K_c is the equilibrium constant which is the ratio of the equilibrium concentration of dye on the adsorbent to that in the solution.

Desorption studies. Desorption experimentations were conducted to analyze the recapture of adsorbent. In each experiment, 0.5 g of CV loaded TGSD was separately agitated with 25 ml of DDDW, 0.1 M hydrochloric acid, 0.1 M sodium chloride, 0.1 M acetic acid, 0.1 M sodium hydroxide and equilibrates for 4 h and then filtered. After filtration, the supernatant was analyzed and percent desorption (%D) was computed by employing the following relation:

$$\%D = \frac{m_d}{m_a} \times 100 \tag{15}$$

where, m_a and m_d represent the concentrations of dye adsorbed and dye desorbed in mg/L, respectively.

Results and Discussion

Adsorbent characterization. The proximate analysis reveals that the TGSD adsorbent contains 5.0% moisture, 0.4% ash, 73.8% volatile matter and 20.8% fixed carbon. The SEM micrographic images of the CV dye unloaded and loaded adsorbent TGSD respectively shown in Fig. 1a,b clearly indicate that the surface of unloaded TGSD is highly irregular, porous and has cave type openings which provide a greater surface area for effective adsorption. After adsorption, the surface of the adsorbent as clearly seen in Fig. 1(b) was altered due to attachment of CV molecules. Obviously, the pores were occupied by CV after adsorption. Thus on the basis of SEM images, it can be inferred that the TGSD adsorbent has adequate morphology for dye adsorption. EDX analysis of TGSD before and after adsorption was carried out to judge the adherence of CV molecules onto the adsorbent surface. The EDX results shown in Fig. 1c,d reflect that the traces of Si and S present in unadsorbed TGSD was replaced by Cl atom of CV ($C_{25}H_{30}ClN_3$). Weight changes in C, N and O atoms were also observed which is clearly due to adsorption of the dye molecule.

The existence of different functional groups on the surface of TGSD was determined by FTIR spectroscopy. The spectrum of TGSD adsorbent is also incorporated in Fig. 1 as Fig. 1e. This figure clearly illustrates that TGSD is enriched with a number of functional groups which are available for adsorption of dye. The strong and broad bands from 3600 to 3200 cm^{-1} attributed to the stretching vibration of a hydroxyl group and adsorbed water while the bands in the range of 3000 to 2850 cm^{-1} may correspond to C–H stretching vibration of alkane group[70]. The broadband peak with a rounded tip at 3396 cm^{-1} of TGSD spectrum is attributed to O–H stretching of an alcoholic group of adsorbent. The peak at 2912 cm^{-1} might be due to C–H stretching of an alkane. A weak band at 1730 cm^{-1} is attributed to C=O stretching non-ionic carboxyl groups (–COOH, –COOCH$_3$) of carboxylic acid or its ester and a medium steep band at 1635 cm^{-1} is accounted to C=O stretching of the ionic carboxylic group (–COO$^-$)[71–74]. A clear peak at 1037 cm^{-1} is due to C–N stretching of the amine group[74] or –OH peak of carbohydrate[75]. The participation of respective functional groups during the adsorption is clear from the change in intensity and peak positions in TGSD after adsorption of CV (Fig. 1e, curve ii). It is evidently seen from the figure that there is a shift in peaks from 3396 to 3421, 2912 to 2920, 1635 to 1614 and 1037 to 1023 cm^{-1} after the adsorption. These shifts in peak indicate the involvement of respective functional groups in the adsorption of CV by TGSD. Thus alcoholic and carboxylic groups take active participation in the adsorption of cationic dye. There strong attractive forces involve between the positive centers of CV dye with the negative center of these groups.

The XRD patterns in the 2θ range 5–60° depicted in Fig. 2 indicate that the present adsorbent is low crystalline material. In fact, the XRD pattern of a biomass is routinely amorphous in nature due to the presence of hemicellulose and lignin[73]. However, two broad peaks observed at the 2θ values of 15.3 and 22.3° are due to the crystalline region of cellulose in TGSD. The broad peaks at around 16° and 22° were also reported by other investigators on different woods such as rubber wood sawdust[76], pinewood[77] and *pinus elliotii* plantation wood[78]. Further Fig. 2 clearly indicates that there is no significant change in crystallinity of the TGSD after the adsorption of CV dye. Thus the crystallinity of TGSD is not affected by the adsorption of dye molecules. This observation rules out the possibility of secondary doping[79].

Effect of contact time and initial concentration of dye. Figure 3 shows the influence of TGSD/CV agitation time on adsorption capacity at the different initial concentrations of dye. It can be realized from the figure that removal efficiency (%) increases with contact time and attained equilibrium in 180 min. After which there is no considerable change in adsorption capacity. However, during the initial 25 min, the rapid increase in adsorption capacity is observed which may be due to a greater number of vacant sites available on the boundary layer of TGSD. The slow increase at the later stage was due to a continuous reduction in the vacant sites. Further adsorption of CV became difficult due to the repulsion of solute between solid and bulk phase. After the initial stage adsorption (i.e. after about 25 min.), the surface pores get almost saturated with CV. Therefore, at the later stage of adsorption, the molecules of CV have to traverse farther and deeper into the micropores of the adsorbent which encounters much larger resistance. Figure 4 also suggests that the adsorption capacity increases with the increase in initial dye concentration at any time. This is due to the fact that at the higher initial dye concentration provides a more driving force which accelerates the mass transfer of adsorbate to the adsorbent. Thus the initial dye concentration plays a significant role in the adsorption capacity in any adsorbate-adsorbent system.
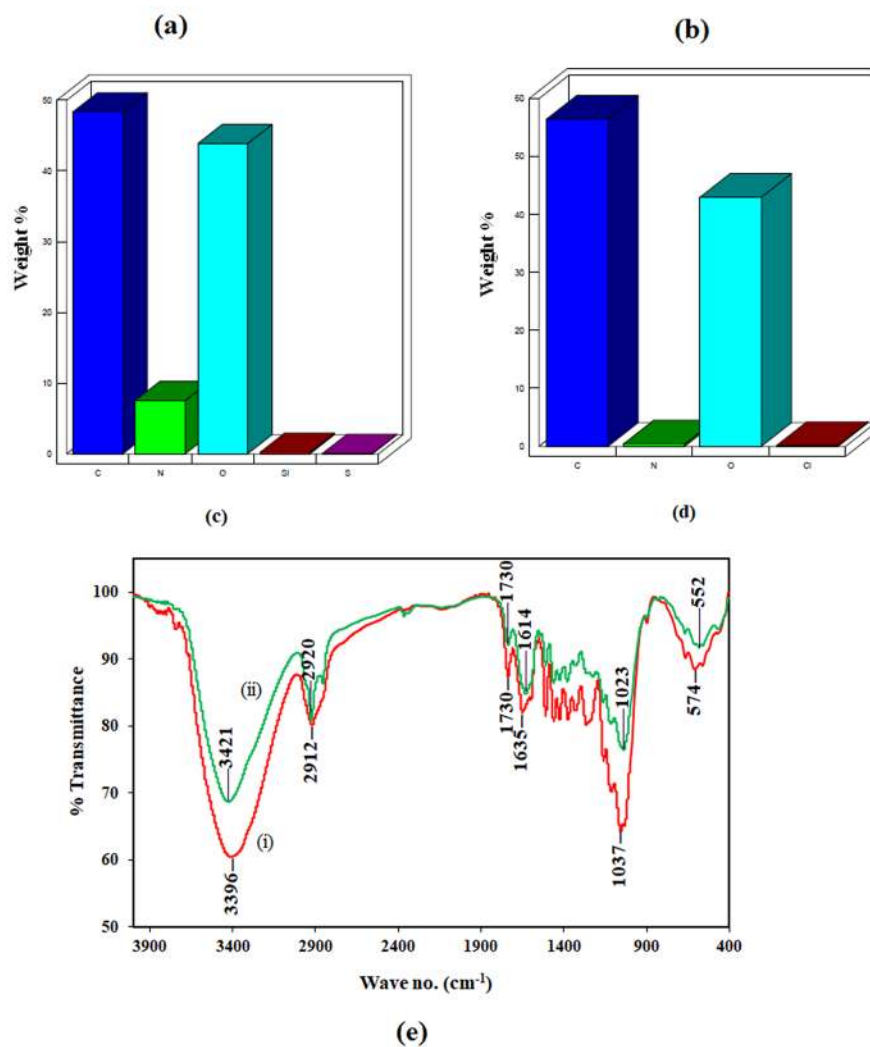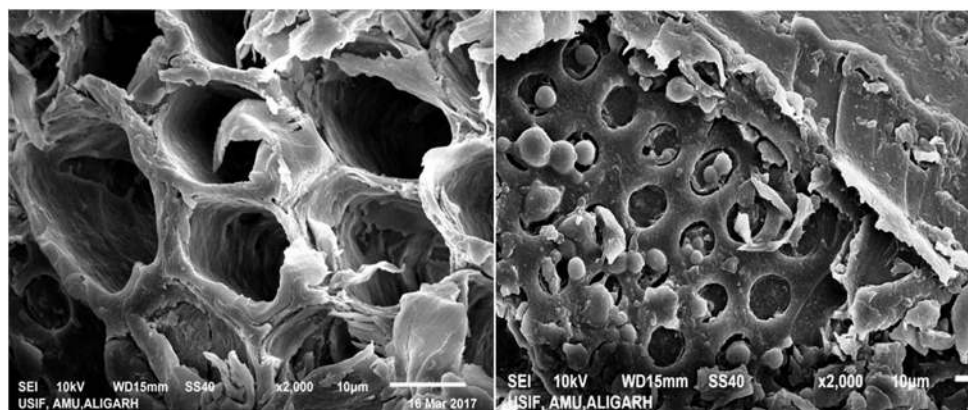
Figure 1. (**a**) SEM micrograph of unloaded TGSD. (**b**) SEM micrograph CV loaded TGSD. (**c**) EDX of unloaded TGSD. (**d**) EDX of CV loaded TGSD. (**e**) FTIR spectra of unloaded and CV loaded TGSD i.e. (i) before and (ii) after adsorption of CV.

Effect of adsorbent dose. The adsorption of CV onto TGSD was studied by changing the adsorbent dose ranging from 0.4 to 12 g/L. The values of adsorption capacity and removal efficiency have been plotted against TGSD dose at the typically chosen experimental conditions of $C_o = 50$ mg/L, temperature = 298 K, contact time = 180 min and pH = 7.5 in Fig. 5. It can be noticeably realized that the removal efficiency increases significantly from 89 to 95% with increased in adsorbent dose from 0.4 to 2.0 g/L and thereafter the increase is relatively slow or insignificant. The increase in removal efficiency with increasing adsorbent dose is due to increase in the overall surface area of the adsorbent and accordingly availability of more binding sites for adsorption. However,
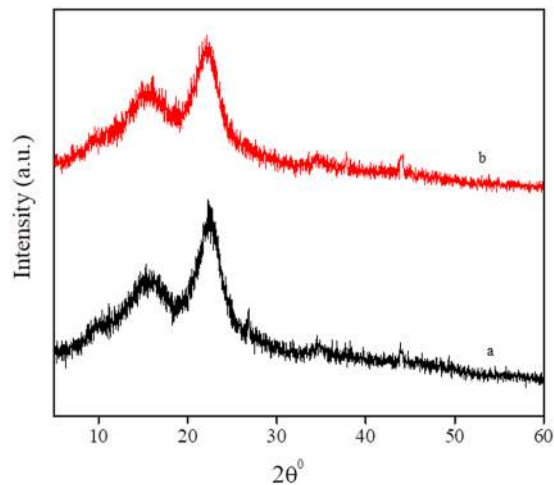
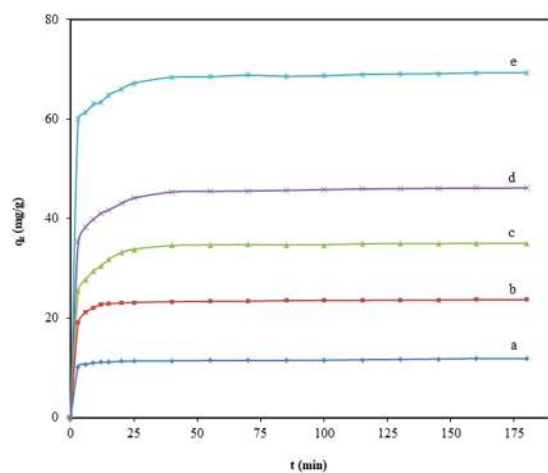**Figure 2.** XRD Spectra (**a**) unloaded TGSD (**b**) CV loaded TGSD.

Figure 3. Effect of contact time on adsorption of CV onto TGSD at different initial dye concentrations: (**a**) 25 mg/L, (**b**) 50 mg/L, (**c**) 75 mg/L, (**d**) 100 mg/L, (**e**) 150 mg/L (experimental conditions: $C_o = 50$ mg/L, temperature = 298 K, adsorbent dose = 2 g/L and pH = 7.5).
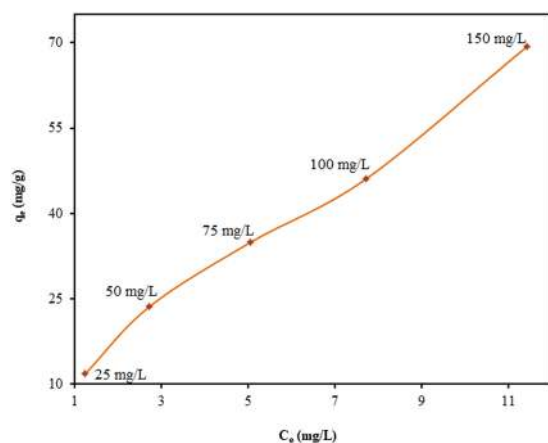

Figure 4. Effect of initial dye concentration on adsorption of CV onto TGSD (experimental conditions: temperature = 298 K, contact time = 180 min, adsorbent dose = 2 g/L and pH = 7.5).
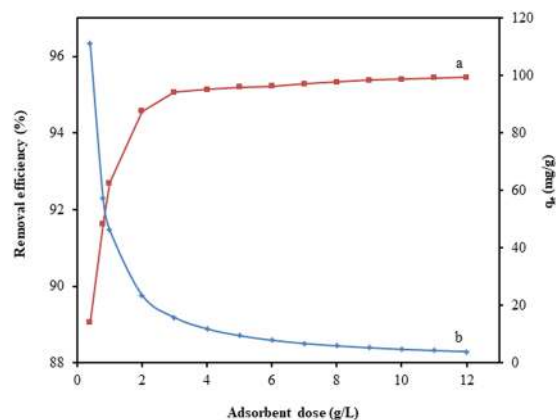
Figure 5. Effect of adsorbent dosage on (**a**) removal efficiency and (**b**) adsorption capacity (experimental conditions: $C_o = 50$ mg/L, temperature $= 298$ K, contact time $= 180$ min and pH $= 7.5$).
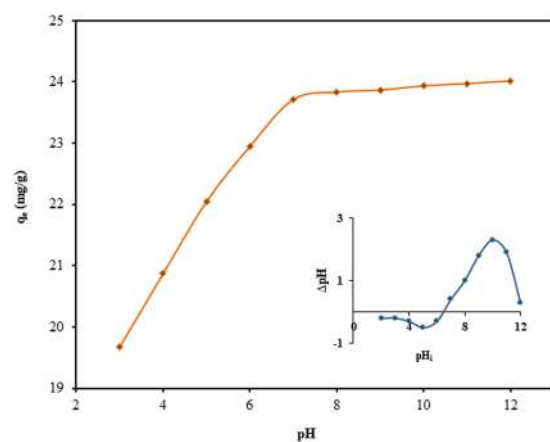

Figure 6. Effect of initial pH on adsorption capacity (inset – determination of the point of zero charge) (experimental conditions: $C_o = 50$ mg/L, temperature $= 298$ K, contact time $= 180$ min and adsorbent dose $= 2$ g/L).

a reverse trend of adsorption capacity has been observed. Figure 5 clearly indicates that the adsorption capacity decreases drastically from 111.0 to 3.9 mg/g with the increase in adsorbent dose from 0.4 to 12.0 g/L. The continuous decrease in adsorption capacity with an increase in TGSD dose is due to the cohesive interaction of adsorbent particles like aggregation or agglomeration which brought about the decrease of the effective surface area per unit weight (g) of the adsorbent and increase in diffusion path length. In view of both positive and negative aspects of increasing adsorbent dose towards removal efficiency and adsorption capacity, a judicious value of 2.0 g/L of the adsorbent dose has been selected for further studies. This adsorbent dose corresponds to a removal efficiency of 94.6% and adsorption capacity of 23.74 mg/g at the initial dye concentration of 50 mg/L.

Effect of pH. The pH of the medium is a significant parameter for adsorption of dye, as it controls the surface charge of the adsorbent as well as the degree of ionization of the solute. The effect of pH was studied by changing the pH of CV solution from 3 to 12. The effect of pH on the adsorption capacity at the experimental conditions of $C_o = 50$ mg/L, temperature $= 298$ K, contact time $= 180$ min and adsorbent dose $= 2.0$ g/L, has been plotted in Fig. 6. This figure clearly indicates that as the pH of the medium is increased from 3 to 7, the value of q_e has been observed to increase drastically, due to increasing electrostatic attraction between cationic CV dye and TGSD surface. In this context, it is relevant to comment that with the increase of pH there is an increase in negative charge of the TGSD surface which causes deprotonating of the functional group present on the adsorbent. Hence, these deprotonated functional groups serve as the binding sites for the cationic CV and cause better adsorption. The lower adsorption of dye in acidic medium is apparently due to electrostatic repulsion of the positively charged adsorbent surface with cationic CV dye. The profound influence of pH on the adsorption can be explained in a better way by an adsorbent characteristic known as the point of zero charge (pH_{pzc}).

The pH_{pzc} of TGSD adsorbent, measured by employing solid-addition method[80], was found to be 6.5 (Fig. 6 – inset). This indicates that at pH < 6.5 the surface has a positive charge due to the protonation, whereas, at pH > 6.5, the adsorbent surface acquires negative charged due to deprotonating in the excess of hydroxyl ions[81]. Thus a value of 6.5 for pH_{pzc} further indicates that the TGSD adsorbent favourably adsorbed any cationic dye at

Particle size (BSS mesh)	% R
80–150	95.1
150–200	98.8
>200	99.6

Table 1. Effect of particle size on removal efficiency (experimental conditions: $C_o = 50$ mg/L, temperature = 298 K, contact time = 180 min, adsorbent dose = 2.0 g/L, pH = 7.5).

Isotherm models	Parameters	Values	R^2
Langmuir	q_m (mg/g)	131.58	
	K_L (L/mg)	0.038	0.998
	R_L	0.345	
Freundlich	n	1.2994	
	K_F ($mg^{1-1/n}L^{1/n}/g$)	10.31	0.989
Temkin	B	22.784	
	K_T (L/g)	0.565	0.961

Table 2. Langmuir, Freundlich, Temkin constant for the adsorption of CV onto TGSD (experimental conditions: temperature = 298 K, contact time = 180 min, adsorbent dose = 2 g/L, pH = 7.5).
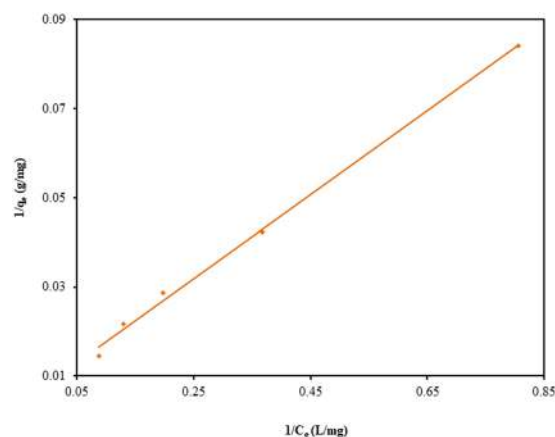

Figure 7. Langmuir adsorption isotherm for the adsorption of CV onto TGSD (experimental conditions: temperature = 298 K, contact time = 180 min, adsorbent dose = 2 g/L, and pH = 7.5).

pH of the medium greater than this value. In view of the above facts, an optimum pH value of 7.5 was chosen for further investigation.

Effect of particle size. Experiments on the adsorptive decontamination CV by TGSD adsorbent were conducted by taking three different size fractions of TGSD powder (80–150, 150–200 and >200 BSS mesh) and the outcomes are incorporated in Table 1. This table demonstrates that as the particle size is decreased from 80–150 BSS to >200 BSS range, the removal efficiency increases from 95.1 to 99.6%. The increase in removal efficiency with decreasing particle size is due to increase in the effective surface area of adsorbent in the same order. However, due to the problems in handling the smaller particle size, particles of 80–150 BSS size fraction were selected throughout the further experiments.

Adsorption isotherm. The isotherm modelling is very significant for the design of any adsorbate-adsorbent system. The present equilibrium results have been fitted to three different isotherm models, namely, Langmuir, Freundlich, and Temkin. The different isotherm parameters based on these models for the adsorption of CV by TGSD have been summarized in Table 2. On comparing the R^2 values so obtained for these models, it has been established that the Langmuir model is best-fitted one. Table 2 openly indicates that our isotherm results are best represented by Langmuir model. The linear form of Langmuir isotherm (equation (7)) plotted in Fig. 7 (experimental conditions: temperature = 298 K, contact time = 180 min, adsorbent dose = 2.0 g/L and pH = 7.5) clearly indicated the excellent validity of this isotherm in CV-TGSD adsorbate-adsorbent system. Thus the adsorption of CV onto TGSD is associated with the monolayer coverage and the adsorbent surface possesses a finite number of adsorption sites with constant energy of adsorption. The validity of Langmuir isotherm also confirms that no further adsorption is possible once the adsorption occurs at the active sites of adsorbent. The favorability of the adsorption has been confirmed by evaluating the R_L value. A value of 0.345 for this parameter confirms that the

Adsorbent	Dose (g/L)	K_L (L/mg)	q_m (mg/g)	R^2
Agaricus bisporous[83]	4	0.15	82.98	1.0
Ananas comosus[84]	2	0.861	78.227	0.999
Breadfruit skin[85]	—	7.35×10^{-5}	145.8	0.9922
Calotropis procera peel[86]	10	0.1139	4.14	—
Cucumis sativus[87]	4	0.076	33.22	0.995
Cucumis sativus/H_2SO_4[87]	4	0.216	35.33	0.989
Eggshell[88]	30	1.341	70.032	0.997
Formosa papaya seed powder[89]	12	0.0015	85.99	0.986
Grapefruit peel[71]	1	0.131	249.68	0.994
Jackfruit leaf powder[90]	10	2.786	43.39	0.999
Jalshakti polymer[91]	0.8	2.22	12.9	0.98
Jute fiber carbon[92]	1	0.227	27.999	0.956
Natural clay mineral[93]	0.5	0.0162	330	0.96
Rice husk/NaOH[94]	10	5.632	44.87	0.992
Sawdust[95]	—	0.68	37.83	0.99
Syzygium cumini leaves[96]	2	3.739	38.750	0.9944
Tea dust[45]	10	0.032	175.4	0.98
Tomato plant root[97]	40	0.02	94.34	0.9918
Water hyacinth[98]	1	0.688	322.58	0.964
Tectona grandis Sawdust (Present study)	2	0.038	131.58	0.998

Table 3. Langmuir isotherm values for the adsorption of CV onto the different adsorbent.

Kinetic models	Parameters	Values	R^2
Pseudo-first-order	K_1 (min^{-1})	0.0246	0.9009
	$q_{e,exp}$ (mg/g)	23.74	
	$q_{e, cal}$ (mg/g)	1.76	
Pseudo-second-order	K_2 (g /min mg)	0.0565	1.000
	$q_{e\ exp}$ (mg/g)	23.74	
	$q_{e\ cal}$ (mg/g)	23.81	
Intraparticle diffusion	k_{id} (mg min$^{-1/2}$/g)	0.2237	0.5261
	C (mg/g)	21.277	

Table 4. Kinetic parameters for the adsorption of CV onto TGSD (experimental conditions: $C_o = 50$ mg/L, temperature $= 298$ K, adsorbent dose $= 2$ g/L, pH $= 7.5$).

adsorption of CV on TGSD is favourable. Further, a value of 0.7696 for 1/n as obtained from Freundlich isotherm clearly indicate a normal Langmuir isotherm and ruled out the possibility of cooperative adsorption[82]. Literature survey reveals that adsorptive decontamination of CV by other adsorbents such as agaricus bisporous[83], ananas comosus[84], breadfruit skin[85], calotropis procera peel[86], cucumis sativus and cucumis sativus/H_2SO_4-modified[87], eggshell[88], formosa papaya seed powder[89], grapefruit peel[71], jackfruit leaf powder[90], jalshakti polymer[91], jute fibre carbon[92], natural clay mineral[93], rice husk/NaOH-modified[94], sawdust[95], syzygium cumini leaves[96], tea dust[45], tomato plant root[97], water hyacinth[98] has also been observed to follow Langmuir isotherm. The values of isotherm constants of this model as reported for different adsorbents are listed in Table 3. This table clearly indicates that there is a large variation in the Langmuir adsorption capacity (q_m) obtained by different investigators. In fact, the maximum monolayer adsorption capacity is strongly dependent on the experimental conditions. For example, the effect of adsorbent dose on the adsorption capacity is highly remarkable (Fig. 5). From Table 3 it may safely be inferred that the TGSD is one of the most prominent and effective adsorbents for the decolorization of wastewater.

Adsorption kinetics. The kinetic results so obtained in the present investigation have been fitted on the pseudo-first-order, pseudo-second-order and intraparticle diffusion models and the relevant parameters associated with these models are incorporated in Table 4. The values of correlation coefficient R^2 linked with different kinetic models clearly tell that the experimental results can be best represented by the pseudo-second-order kinetic model. The plot of experimental results (t/q_t against t) for pseudo-second-order kinetics for different initial dye concentrations shown in Fig. 8 lead to the straight line with the excellent correlation coefficient values ranging from 0.9998 to 1.0. The calculated values of pseudo-second-order kinetic parameters for the initial dye concentration of 50 mg/L have been incorporated in Table 4. This table indicates that the experimental value of adsorption capacity (23.74 mg/g) is in a very close agreement with the value of 23.81 mg/g as calculated
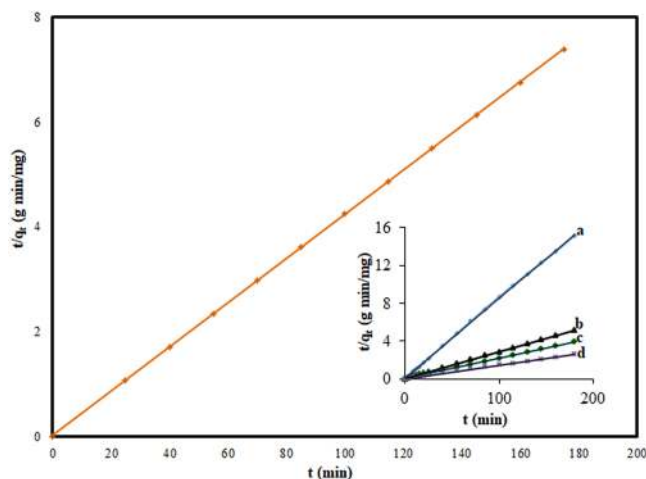
Figure 8. Pseudo-second order kinetic plot the adsorption of CV onto TGSD at concentration of 50 mg/L ($R^2 = 1$) (inset – at different concentrations: (**a**) 25 mg/L ($R^2 = 0.9998$) (**b**) 75 mg/L ($R^2 = 0.9999$) (**c**) 100 mg/L ($R^2 = 1$) (**d**) 150 mg/L ($R^2 = 1$) (experimental conditions: $C_o = 50$ mg/L, temperature = 298 K, adsorbent dose = 2 g/L, and pH = 7.5).

Adsorbent	K_2 (g/min mg)	q_{cal} (mg/g)	R^2
Agaricus bisporous[83]	0.15	19.18	1.000
Alligator weed[99]	2.6×10^2	14.5	0.99
Ananas comosus[84]	0.00625	74.262	0.992
breadfruit skin[85]	0.061	118.31	0.9056
Cucumis sativus[87]	0.04	12.077	0.9999
Cucumis sativus/H_2SO_4[87]	0.019	12.091	0.9956
Eggshell[88]	0.00725	68.056	0.9996
Formosa papaya seed powder[89]	0.078	1.890	0.993
Grapefruit peel[71]	0.005	24.31	0.992
Jackfruit leaf powder[90]	0.0193	39.45	0.999
Jute fiber carbon[92]	0.004	19.164	0.998
Laminaria japonica[99]	0.7×10^2	16.1	0.99
Rice bran[99]	1.9×10^2	15.2	0.99
Rice husk/NaOH[94]	0.00234	42.053	0.998
Sawdust[95]	0.0017	28.74	0.998
Syzygium cumini leaves[96]	0.014	51.020	0.9368
Tea dust[45]	0.002	45.46	0.9999
Water hyacinth[98]	0.05	434.78	1
Wheat bran[99]	0.8×10^2	15.8	0.99
Tectona grandis Sawdust (Present study)	0.0565	23.81	1.000

Table 5. Pseudo-second-order kinetic parameters for adsorption of CV onto different adsorbents.

by employing pseudo-second-order equation. This again confirms that the kinetics of CV-TGSD system obeys pseudo-second-order model.

This model has also been reported to be followed by the adsorption of CV onto other similar adsorbents, namely, agaricus bisporous[83], alligator weed[99], ananas comosus[84], breadfruit skin[85], cucumis sativus and cucumis sativus/H_2SO_4-modified[87], eggshell[88], formosa papaya seed powder[89], grapefruit peel[71], jackfruit leaf powder[90], jute fibre carbon[92], laminaria japonica[99], rice bran[99], rice husk/NaOH-modified[94], sawdust[95], syzygium cumini leaves[96], tea dust[45], water hyacinth[98] and wheat bran[99]. The different kinetic parameters obtained by these investigators have been compared with those of present study in Table 5. This table clearly indicates that our value of 0.0565 g/min mg for the Pseudo-second-order rate constant (K_2) falls under the comparable range of literature values (0.0017–0.15 g/min mg).

Adsorption thermodynamics. The values of $\Delta G°$ calculated by using equation (13) and other thermodynamic parameters, namely, $\Delta H°$ and $\Delta S°$ as generated from ln K_c vs 1/T plot shown in Fig. 9 are presented in Table 6. The adsorption process has been observed to be accompanied by the decrease in free energy throughout
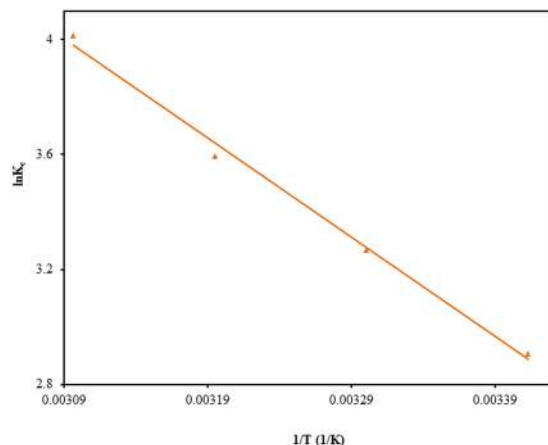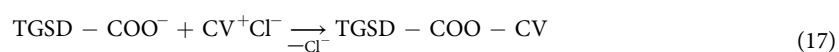
10

Figure 9. Plot of ln K_c vs 1/T for the adsorption of CV onto TGSD adsorbent (experimental conditions: $C_o = 50$ mg/L, contact time = 180 min, adsorbent dose = 2 g/L, and pH = 7.5).

Temperature (K)	$-\Delta G_o$ (kJ/mol)	ΔH_o (kJ/mol)	ΔS_o (J/K mol)
293	7.080		
303	8.230	28.642	121.8
313	9.352		
323	10.776		

Table 6. Thermodynamic parameters for the adsorption of CV onto TGSD (experimental conditions: $C_o = 50$ mg/L, contact time = 180 min, adsorbent dose = 2.0 g/L, pH = 7.5).

the entire temperature range. This reveals that the adsorption of CV by TGSD is feasible. This table shows that the negative values of free energy change increase with the increase of temperature. This shows that the spontaneity of the adsorption increases with the rise of temperature. The positive value enthalpy change specifies that the adsorption is endothermic and accompanying with the absorption of heat from the surroundings. Hence the feasibility of the adsorption depends solely on the increase of entropy during adsorption CV by TGSD. A positive value of 121.8 J/K mol shows that there is an increase in disorder at the adsorbate/adsorbent interface. The enhancement in entropy is due to displacement of the coordinated water molecule by the dye molecules which resulted in a gain of more translational entropy than the lost by dye molecules[100]. This increase in disorder or randomness provides the driving force for the adsorption. Literature survey reveals that increase in randomness has also been observed for removal of CV by other adsorbents, such as alligator weed[99], bottom ash[16], deoiled soya[16], lignified elephant grass complexed isolate[101], laminaria japonica[99], natural clay mineral[93], rice bran[99], terminalia arjuna sawdust[102], tomato plant root[97] water hyacinth[98], wheat bran[99], etc.

Adsorption mechanism. The FTIR analysis has indicated the presence of polar hydroxyl, carboxyl and amine groups in TGSD. It has been pointed out that the adsorption of cationic dyes is mainly due to –OH and –COO$^-$ functional groups[72]. Thus the adsorption of CV onto TGSD might be owing to the strong electrostatic attraction of these groups with the charged centers of cationic CV (CV$^+$Cl$^-$) molecules. Further at higher pH (i.e. > pH$_{pzc}$), the OH$^-$ ions accumulate on the surface of TGSD and accordingly the surface acquires a negative charge. In the present investigation, the adsorption of CV by TGSD was found to be strongly pH dependent (Fig. 6) and the favourable pH of the solution for CV adsorption was ranging from 7 to 12. Thus the adsorption capacity becomes significant at higher pH due to electrostatic attraction between negatively charge adsorbent surface and cationic CV molecules. The attachment of CV on TGSD occurred due to electrostatic attraction of cationic dye with the negatively charged adsorbent containing the above mentioned functional groups (–OH and –COO$^-$). The adsorption of CV molecules on TGSD adsorbent may be mechanistically represented as:

$$\text{TGSD} - \text{OH} \xrightarrow[-\text{H}_2\text{O}]{\text{OH}^-} \text{TGSD} - \text{O}^- \xrightarrow[-\text{Cl}^-]{\text{CV}^+\text{Cl}^-} \text{TGSD} - \text{O} - \text{CV} \tag{16}$$

$$\text{TGSD} - \text{COO}^- + \text{CV}^+\text{Cl}^- \xrightarrow[-\text{Cl}^-]{} \text{TGSD} - \text{COO} - \text{CV} \tag{17}$$

In the above possible reactions, the cationic CV dye ($C_{25}N_3H_{30}Cl$) is written as CV$^+$Cl$^-$. The suggested mechanism is reinforced by the experimental observation of the poor adsorption at lower pH. At the lower pH i.e. under acidic condition, the generation of Cl$^-$ ions would be suppressed resulting the overall suppress of adsorption due to carboxylate ion of the adsorbent. This proposed mechanism based on the electrostatic force between positive
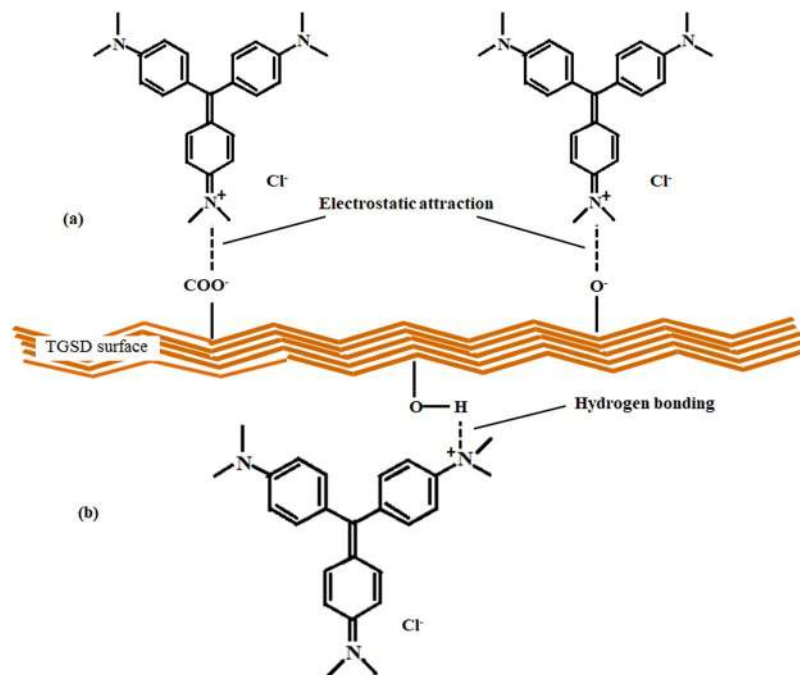
Figure 10. Proposed plausible interaction of crystal violet dye on TGSD Adsorbent.

Desorbing agent	% Desorption
HCL	33.37
CH$_3$COOH	18.94
NaOH	5.86
NaCl	3.62
DDW	1.40

Table 7. Percentage desorption of CV from CV loaded TGSD.

centers of CV and –OH/–COO$^-$ groups of adsorbent has been graphically presented in Fig. 10(a). The similar mechanism based on the electrostatic attraction between –COO$^-$ of grapefruit peel and positive N site of CV dye has already been proposed[71].

Furthermore, in addition to the involvement of the attractive forces between the cationic site of CV and –OH/–COO$^-$ functional groups of TGSD, the involvement of the possible hydrogen bonds between alcoholic –OH group of adsorbent and amine group of adsorbate CV is quite justified. The possible formation of hydrogen bonding is illustrated in Fig. 10(b). In this context, it is relevant to mention here that the adsorption of CV on the surface of NaOH modified rice husk was suggested by the involvement of hydrogen bonding between the –OH groups on the rice husk surface and the nitrogen atoms of CV[94] as similar as proposed in Fig. 10(b).

The probability of intraparticle pore diffusion of CV can be judged by intraparticle diffusion kinetic model. It has been suggested that the q_t vs $t^{\frac{1}{2}}$ plot should linear and pass through the origin if the intraparticle diffusion is the only rate-limiting step[103]. But in the present case, a positive intercept of 21.277 mg/g (Table 4) was observed which showed that the dye removal kinetics may be governed by both film diffusion and intraparticle diffusion together[103,104].

Thus on the basis of the above findings, the adsorption mechanism of CV onto TGSD can safely to be assumed to be involved in the following consecutive steps: (i) movement of CV molecules from the solution bulk to the surface of the TGSD, (ii) diffusion of CV molecules through the boundary layer to the surface of TGSD adsorbent, and (iii) adsorption of CV on the surface of TGSD by the (a) electrostatic attractive force between polar groups (–OH and –COO$^-$) of TGSD and charged centers of CV (CV$^+$Cl$^-$) molecules and (b) strong hydrogen bonding between the hydroxyl group of TGSD and amine group of CV.

Desorption. The possible regeneration of used TGSD adsorbent was explored by conducting desorption studies with different desorbing agents (0.1 M HCl, 0.1 M CH$_3$COOH, 0.1 M NaCl, 0.1 M NaOH and DDDW) and the results are summarised in Table 7. The maximum desorption (33.37%) of CV was observed with hydrochloric acid. Thus in order to increase the desorption i.e. better utility adsorbent and economic feasibility of the process, further work is needed in this direction.

Conclusions

The present investigation reflects that *Tectona grandis* sawdust (TGSD) is an efficient adsorbent for the decontamination of crystal violet (CV) dye from wastewater. It was observed that the adsorption capacity was influenced by different investigational variables like contact time, adsorbent dose, pH, the concentration of dye and temperature. The adsorption capacity was observed to be increased with increasing pH of the medium up to a value of 7 and thereafter it remains almost stagnant on a further increase of pH. Equilibrium time for adsorption of CV onto TGSD was found to be 180 min. Kinetic study revealed that adsorption was best described by pseudo-second-order kinetics. Adsorption equilibrium data were found to be best fitted by Langmuir isotherm model suggesting that the adsorption occurred in a monolayer manner on the homogeneous adsorbent surface having identical sites. The maximum equilibrium adsorption capacity was observed to be 131.58 mg/g which suggested that the present adsorbent is one of the most promising among the adsorbents of the similar category. The high value of equilibrium adsorption capacity clearly suggests that the present method can be successfully exploited to make impure wastewater to be reusable. The thermodynamic study showed that the decontamination of CV by TGSD was spontaneous, endothermic and associated with an increase in entropy. The desorption of TGSD from CV loaded TGSD for reuse was observed to be highest with 0.1 M HCl. The exhaustive studies indicated that the TGSD is one of the most prominent and effective adsorbents, for the decontamination of CV polluted wastewater, among the other adsorbents of similar category.

References

1. Ahmed, T., Imdad, S., Yaldram, K., Butt, N. M. & Pervez, A. Emerging nanotechnology-based methods for water purification: a review. *Desalin. Water Treat.* **52**, 4089–4101 (2014).
2. Kar, D., Sur, P., Mandai, S. K., Saha, T. & Kole, R. K. Assessment of heavy metal pollution in surface water. *Int. J. Environ. Sci. Technol.* **5**, 119–124 (2008).
3. Jadhav, J. P., Kalyani, D. C., Telke, A. A., Phugare, S. S. & Govindwar, S. P. Evaluation of the efficacy of a bacterial consortium for the removal of color, reduction of heavy metals, and toxicity from textile dye effluent. *Bioresource Technol.* **101**, 165–173 (2010).
4. Qamruzzaman & Nasar, A. Degradation of acephate by colloidal manganese dioxide in the absence and presence of surfactants. *Desalin. Water Treat.* **55**, 2155–2164 (2015).
5. Schwarzenbach, R. P., Egli, T., Hofstetter, T. B., von Gunten, U. & Wehrli, B. Global water pollution and human health. *Annu. Rev. Environ. Resour.* **35**, 109–136 (2010).
6. Jarup, L. Hazards of heavy metal contamination. *Brit. Med. Bull.* **68**, 167–182 (2003).
7. Prüss-Ustün, A., Vickers, C., Haefliger, P. & Bertollini, R. Knowns and unknowns on burden of disease due to chemicals: a systematic review. *Environ. Health.* **10**, 9 (2011).
8. Tsuboy, M. S. *et al.* Genotoxic, mutagenic and cytotoxic effects of the commercial dye CI disperse blue 291 in the human hepatic cell line HepG2. *Toxicol. Vitro.* **21**, 1650–1655 (2007).
9. Barbosa, P. & Peters, T. M. The effects of vital dyes on living organisms with special reference to methylene blue and neutral red. *Histochem. J.* **3**, 71–93 (1971).
10. Cassano, A., Molinari, R., Romano, M. & Drioli, E. Treatment of aqueous effluents of the leather industry by membrane processes. *J. Membrane Sci.* **181**, 111–126 (2001).
11. Kant, R. Textile dyeing industry an environmental hazard. *Nat. Sci.* **4**, 22–26 (2012).
12. Verma, A. K., Dash, R. R. & Bhunia, P. A review on chemical coagulation/flocculation technologies for removal of colour from textile wastewaters. *J. Environ. Manage.* **93**, 154–168 (2012).
13. Crini, G. Non-conventional low-cost adsorbents for dye removal: a review. *Bioresource Technol.* **97**, 1061–1085 (2006).
14. Mani, S. & Bharagava, R. N. Exposure to crystal violet, its toxic, genotoxic and carcinogenic effects on environment and its degradation and detoxification for environmental safety. *Rev. Environ. Contam. Toxicol.* **237**, 71–104 (2016).
15. Forgacs, E., Cserháti, T. & Oros, G. Removal of synthetic dyes from wastewaters: a review. *Environ. Int.* **30**, 953–971 (2004).
16. Mittal, A., Mittal, J., Malviya, A., Kaur, D. & Gupta, V. K. Adsorption of hazardous dye crystal violet from wastewater by waste materials. *J. Colloid Interface Sci.* **343**, 463–473 (2010).
17. Brown, D. Effects of colorants in the aquatic environment. *Ecotoxicol. Environ. Safety.* **13**, 139–147 (1987).
18. Deshannavar, U. B. *et al.* Optimization, kinetic and equilibrium studies of disperse yellow 22 dye removal from aqueous solutions using malaysian teak wood sawdust as adsorbent. *Indian. Chem. Eng.* **58**, 12–28 (2016).
19. Nasar, A. & Shakoor, S. Remediation of dyes from industrial wastewater using low-cost adsorbents. In *Applications of Adsorption and Ion Exchange Chromatography in Waste Water Treatment* (eds Inamuddin & Al-Ahmed, A.) 1–33, https://doi.org/10.21741/9781945291333-1 (Materials ResearchForum LLC, 2017).
20. Korngold, E., Kock, K. & Strathmann, H. Electrodialysis in advanced waste water treatment. *Desalination* **24**, 129–139 (1977).
21. Bahnemann, D. Photocatalytic water treatment: solar energy applications. *Solar Energ.* **77**, 445–459 (2004).
22. Chong, M. N., Jin, B., Chow, C. W. K. & Saint, C. Recent developments in photocatalytic water treatment technology: a review. *Water Res.* **44**, 2997–3027 (2010).
23. Ivnitsky, H. *et al.* Bacterial community composition and structure of biofilms developing on nanofiltration membranes applied to wastewater treatment. *Water Res.* **41**, 3924–3935 (2007).
24. Ahmad, A. L., Tan, L. S. & Shukor, S. R. A. Dimethoate and atrazine retention from aqueous solution by nanofiltration membranes. *J. Hazard. Mater.* **151**, 71–77 (2008).
25. Chen, X., Chen, G. & Yue, P. L. Novel electrode system for electroflotation of wastewater. *Environ. Sci. Technol.* **36**, 778–783 (2002).
26. Wang, A., Qu, J., Liu, H. & Ge, J. Degradation of azo dye acid red 14 in aqueous solution by electrokinetic and electrooxidation process. *Chemosphere* **55**, 1189–1196 (2004).
27. Butani, S. A. & Mane, S. J. Coagulation/flocculation process for cationic, anionic dye removal using water treatment residuals – a review. *Int. J. Sci. Technol. Mange.* **6**, 121–125 (2017).
28. Amuda, O. & Amoo, I. Coagulation/flocculation process and sludge conditioning in beverage industrial wastewater treatment. *J. Hazard. Mater.* **141**, 778–783 (2007).
29. Wang, J.-P., Chen, Y.-Z., Ge, X.-W. & Yu, H.-Q. Optimization of coagulation–flocculation process for a paper-recycling wastewater treatment using response surface methodology. *Colloid. Surface. A.* **302**, 204–210 (2007).
30. Greenlee, L. F., Lawler, D. F., Freeman, B. D., Marrot, B. & Moulin, P. Reverse osmosis desalination: water sources, technology, and today's challenges. *Water Res.* **43**, 2317–2348 (2009).
31. Lin, S. H. & Lin, C. M. Treatment of textile waste effluents by ozonation and chemical coagulation. *Water Res.* **27**, 1743–1748 (1993).
32. Schröder, H. F. Non-biodegradable wastewater compounds treated by ozone or ozone/UV — conversion monitoring by substance-specific analysis and biotoxicity testing. *Water Sci.Technol.* **33** (1996).

33. Qamruzzaman & Nasar, A. Degradative treatment of bispyribac sodium herbicide from synthetically contaminated water by colloidal MnO₂ dioxide in the absence and presence of surfactants. *Environ. Technol.* 1–7, https://doi.org/10.1080/09593330.2017.1396500 (2017).
34. Qamruzzaman & Nasar, A. Treatment of acetamiprid insecticide from artificially contaminated water by colloidal manganese dioxide in the absence and presence of surfactants. *RSC Adv.* **4**, 62844–62850 (2014).
35. Qamruzzaman & Nasar, A. Kinetics of metribuzin degradation by colloidal manganese dioxide in absence and presence of surfactants. *Chem. Pap.* **68**, 65–73 (2014).
36. Qamruzzaman & Nasar, A. Degradation of tricyclazole by colloidal manganese dioxide in the absence and presence of surfactants. *J. Ind. Eng. Chem.* **20**, 897–902 (2014).
37. Velickovic, T. C., Ognjenovic, J. & Mihajlovic, L. Separation of Amino Acids, Peptides, and Proteins by Ion Exchange Chromatography. *Ion Exc. Technol. II: Applications* (eds Inamuddin, D. & Luqman, M.) 1–34, https://doi.org/10.1007/978-94-007-4026-6_1 (Springer Netherlands, 2012).
38. Chan, Y. J., Chong, M. F., Law, C. L. & Hassell, D. G. A review on anaerobic–aerobic treatment of industrial and municipal wastewater. *Chem. Eng. J.* **155**, 1–18 (2009).
39. Bhatnagar, A. & Sillanpää, M. Utilization of agro-industrial and municipal waste materials as potential adsorbents for water treatment—a review. *Chem. Eng. J.* **157**, 277–296 (2010).
40. Nasar, A. Polyaniline (PANI) based composites for the adsorptive treatment of polluted water. In *Smart Polymers and Composites* (ed. Nasar, A.) 41–64, https://doi.org/10.21741/9781945291470-2 (Materials Research Foundations, 2018).
41. Nasuha, N., Hameed, B. H. & Din, A. T. M. Rejected tea as a potential low-cost adsorbent for the removal of methylene blue. *J. Hazard. Mater.* **175**, 126–132 (2010).
42. Anastopoulos, I., Bhatnagar, A., Hameed, B. H., Ok, Y. S. & Omirou, M. A review on waste-derived adsorbents from sugar industry for pollutant removal in water and wastewater. *J. Mol. Liq.* **240**, 179–188 (2017).
43. Lee, J.-W., Choi, S.-P., Thiruvenkatachari, R., Shim, W.-G. & Moon, H. Evaluation of the performance of adsorption and coagulation processes for the maximum removal of reactive dyes. *Dye. Pigment.* **69**, 196–203 (2006).
44. Deaconu, M. & Senin, R. Adsorption decolorization technique of textile/leather – dye containing effluents. *Int. J. Waste. Resour.* **6**, (2016).
45. Khan, M. M. R., Rahman, M. W., Ong, H. R., Ismail, A. B. & Cheng, C. K. Tea dust as a potential low-cost adsorbent for the removal of crystal violet from aqueous solution. *Desalin. Water Treat.* **57**, 14728–14738 (2016).
46. Tanweer *et al.* Oil Palm Biomass–Based adsorbents for the removal of water pollutants—a Review. *J. Environ. Sci. Heal. C.* **29**, 177–222 (2011).
47. Tahir, H., Sultan, M., Akhtar, N., Hameed, U. & Abid, T. Application of natural and modified sugar cane bagasse for the removal of dye from aqueous solution. *J. Saudi. Chem. Soc.* **20**, S115–S121 (2016).
48. Shakoor, S. & Nasar, A. Removal of methylene blue dye from artificially contaminated water using *Citrus limetta* peel waste as a very low cost adsorbent. *J. Taiwan Inst. Chem. E.* **66**, 154–163 (2016).
49. Shakoor, S. & Nasar, A. Adsorptive treatment of hazardous methylene blue dye from artificially contaminated water using *Cucumis sativus* peel waste as a low-cost adsorbent. *Groundwater for Sustainable Development* **5**, 152–159 (2017).
50. Garg, V. Basic dye (methylene blue) removal from simulated wastewater by adsorption using indian rosewood sawdust: a timber industry waste. *Dye. Pigment.* **63**, 243–250 (2004).
51. Namasivayam, C., Jeyakumar, R. & Yamuna, R. T. Dye removal from wastewater by adsorption on 'waste' Fe(III)/Cr(III) hydroxide. *Waste Manage.* **14**, 643–648 (1994).
52. Messina, P. V. & Schulz, P. C. Adsorption of reactive dyes on titania–silica mesoporous materials. *J. Colloid Interface Sci.* **299**, 305–320 (2006).
53. Ozdemir, O., Armagan, B., Turan, M. & Çelik, M. S. Comparison of the adsorption characteristics of azo-reactive dyes on mezoporous minerals. *Dye. Pigment.* **62**, 49–60 (2004).
54. Armağan, B., Turan, M. & Ęlik, M. S. Equilibrium studies on the adsorption of reactive azo dyes into zeolite. *Desalination* **170**, 33–39 (2004).
55. Cardoso, N. F. *et al.* Application of cupuassu shell as biosorbent for the removal of textile dyes from aqueous solution. *J. Environ. Manage.* **92**, 1237–1247 (2011).
56. Iqbal, J. *et al.* Adsorption of acid yellow dye on flakes of chitosan prepared from fishery wastes. *Arab. J. Chem.* **4**, 389–395 (2011).
57. Annadurai, G., Ling, L. Y. & Lee, J.-F. Adsorption of reactive dye from an aqueous solution by chitosan: isotherm, kinetic and thermodynamic analysis. *J. Hazard. Mater.* **152**, 337–346 (2008).
58. Wu, F.-C., Tseng, R.-L. & Juang, R.-S. Characteristics of elovich equation used for the analysis of adsorption kinetics in dye-chitosan systems. *Chem. Eng. J.* **150**, 366–373 (2009).
59. Palanisamy, K., Hegde, M. & Jae-Seon, Y. Teak (*Tectona grandis* Linn. f.): A renowned commercial timber species. *J. For. Sci.* **25**, 1–24 (2009).
60. Kwame, O., Adjei, L. E. & Richmond, O. Assessing the growth performance of teak (*Tectona grandis* Linn. f.) coppice two years after clearcut harvesting. *Int. J. Agron. Agric. Res.* **5**, 36–41 (2014).
61. Zainuddin, M. F., Shamsudin, R., Mokhtar, M. N. & Ismail, D. Physicochemical properties of pineapple plant waste fibres from the leaves and stems of different varieties. *Bio. Resour.* **9**, 5311–5324 (2014).
62. Foo, K. Y. & Hameed, B. H. Insights into the modeling of adsorption isotherm systems. *Chem. Eng. J.* **156**, 2–10 (2010).
63. Yang, C. Statistical mechanical study on the freundlich isotherm equation. *J. Colloid Interface Sci.* **208**, 379–387 (1998).
64. Johnson, R. D. & Arnold, F. H. The temkin isotherm describes heterogeneous protein adsorption. *Biochim. Biophys. Acta. Protein Struct. Mol. Enzymol.* **1247**, 293–297 (1995).
65. Ho, Y. S. & McKay, G. A. Comparison of chemisorption kinetic models applied to pollutant removal on various sorbents. *Process Saf. Environ. prot.* **76**, 332–340 (1998).
66. Doğan, M., Özdemir, Y. & Alkan, M. Adsorption kinetics and mechanism of cationic methyl violet and methylene blue dyes onto sepiolite. *Dye. Pigment.* **75**, 701–713 (2007).
67. Ho, Y. S. & McKay, G. Pseudo-second order model for sorption processes. *Process Biochem.* **34**, 451–465 (1999).
68. Vadivelan, V. & Kumar, K. V. Equilibrium, kinetics, mechanism, and process design for the sorption of methylene blue onto rice husk. *J. Colloid Interface Sci.* **286**, 90–100 (2005).
69. Tan, K. L. & Hameed, B. H. Insight into the adsorption kinetics models for the removal of contaminants from aqueous solutions. *J. Taiwan Inst. Chem. E.* **74**, 25–48 (2017).
70. Kalavathy, M. H. & Miranda, L. R. Comparison of copper adsorption from aqueous solution using modified and unmodified *Hevea brasiliensis* saw dust. *Desalination* **255**, 165–174 (2010).
71. Saeed, A., Sharif, M. & Iqbal, M. Application potential of grapefruit peel as dye sorbent: kinetics, equilibrium and mechanism of crystal violet adsorption. *J. Hazard. Mater.* **179**, 564–572 (2010).
72. Pan, X. *et al.* Litchi pericarps used as adsorbents for methylene blue removal from solution. *Desalin. Water Treat.* **55**, 1333–1341 (2015).
73. Basu, M., Guha, A. K. & Ray, L. Adsorption of lead on cucumber peel. *J. Clean. Prod.* **151**, 603–615 (2017).
74. Alizadeh, N., Shariati, S. & Besharati, N. Adsorption of crystal violet and methylene blue on azolla and fig leaves modified with magnetite iron oxide nanoparticles. *Int. J. Environ. Res.* **11**, 197–206 (2017).

75. Das, K. *et al*. FTIR of touch imprint cytology: a novel tissue diagnostic technique. *J. Photochem. Photobiol. B.* **92**, 160–164 (2008).
76. Shaaban, A., Se, S.-M., Mitan, N. M. M. & Dimin, M. F. Characterization of biochar derived from rubber wood sawdust through slow pyrolysis on surface porosities and functional groups. *Procedia Eng.* **68**, 365–371 (2013).
77. Wang, Z., Cao, J. & Wang, J. Pyrolytic characteristics of pine wood in a slowly heating and gas sweeping fixed-bed reactor. *J. Anal. Appl. Pyrol.* **84**, 179–184 (2009).
78. Jiang, Z.-H., Yang, Z., So, C.-L. & Hse, C.-Y. Rapid prediction of wood crystallinity in *Pinus elliotii* plantation wood by near-infrared spectroscopy. *J. Wood Sci.* **53**, 449–453 (2007).
79. Mahanta, D., Madras, G., Radhakrishnan, S. & Patil, S. Adsorption and desorption kinetics of anionic dyes on doped polyaniline. *J. Phys. Chem. B.* **113**, 2293–2299 (2009).
80. Khattri, S. D. & Singh, M. K. Removal of malachite green from dye wastewater using neem sawdust by adsorption. *J. Hazard. Mater.* **167**, 1089–1094 (2009).
81. Malekbala, M. R., Hosseini, S., Yazdi, S. K., Soltani, S. M. & Malekbala, M. R. The study of the potential capability of sugar beet pulp on the removal efficiency of two cationic dyes. *Chem. Eng. Res. Des.* **90**, 704–712 (2012).
82. Fytianos, K., Voudrias, E. & Kokkalis, E. Sorption–desorption behaviour of 2,4-dichlorophenol by marine sediments. *Chemosphere* **40**, 3–6 (2000).
83. Pandey, P., Singh, R. P., Singh, K. N. & Manisankar, P. Evaluation of the individuality of white rot macro fungus for the decolorization of synthetic dye. *Environ. Sci. Pollut. Res.* **20**, 238–249 (2013).
84. Chakraborty, S., Chowdhury, S. & Saha, P. Das. Insight into biosorption equilibrium, kinetics and thermodynamics of crystal violet onto *Ananas comosus* (pineapple) leaf powder. *Appl. Water. Sci.* **2**, 135–141 (2012).
85. Lim, L. B. L., Priyantha, N. & Mansor, N. H. M. *Artocarpus altilis* (breadfruit) skin as a potential low-cost biosorbent for the removal of crystal violet dye: equilibrium, thermodynamics and kinetics studies. *Environ. Earth. Sci.* **73**, 3239–3247 (2015).
86. Ali, H. & Muhammad, S. K. Biosorption of crystal violet from water on leaf biomass of *Calotropis procera*. *J. Environ. Sci. Technol.* **1**, 143–150 (2008).
87. Smitha, T., Santhi, T., Prasad, A. L. & Manonmani, S. *Cucumis sativus* used as adsorbent for the removal of dyes from aqueous solution. *Arab J. Chem.* **10**, S244–S251 (2017).
88. Chowdhury, S., Chakraborty, S. & Saha, P. Das. Removal of crystal violet from aqueous solution by adsorption onto eggshells: equilibrium, kinetics, thermodynamics and artificial neural network modeling. *Waste and Biomass Valorization* **4**, 655–664 (2013).
89. Pavan, F. A. *et al*. Formosa papaya seed powder (FPSP): preparation, characterization and application as an alternative adsorbent for the removal of crystal violet from aqueous phase. *J. Environ. Chem. Eng.* **2**, 230–238 (2014).
90. Saha, P. D., Chakraborty, S. & Chowdhury, S. Batch and continuous (fixed-bed column) biosorption of crystal violet by *Artocarpus heterophyllus* (jackfruit) leaf powder. *Colloid. Surface. B.* **92**, 262–270 (2012).
91. Dhodapkar, R., Rao, N. N., Pande, S. P., Nandy, T. & Devotta, S. Adsorption of cationic dyes on jalshakti®, super absorbent polymer and photocatalytic regeneration of the adsorbent. *React. Funct. Polym.* **67**, 540–548 (2007).
92. Porkodi, K. & Kumar, K. V. Equilibrium, kinetics and mechanism modeling and simulation of basic and acid dyes sorption onto jute fiber carbon: eosin yellow, malachite green and crystal violet single component systems. *J. Hazard. Mater.* **143**, 311–327 (2007).
93. Sakin Omer, O., Hussein, M. A., Hussein, B. H. M. & Mgaidi, A. Adsorption thermodynamics of cationic dyes (methylene blue and crystal violet) to a natural clay mineral from aqueous solution between 293.15 and 323.15 K. *Arab J. Chem*., https://doi.org/10.1016/j.arabjc.2017.10.007 (2017).
94. Chakraborty, S., Chowdhury, S. & Das Saha, P. Adsorption of crystal violet from aqueous solution onto NaOH-modified rice husk. *Carbohyd. Polym.* **86**, 1533–1541 (2011).
95. Parab, H., Sudersanan, M., Shenoy, N., Pathare, T. & Vaze, B. Use of agro-industrial wastes for removal of basic dyes from aqueous solutions. *Clean-Soil, Air, Water* **37**, 963–969 (2009).
96. Mehmood, A., Bano, S., Fahim, A., Parveen, R. & Khurshid, S. Efficient removal of crystal violet and eosin B from aqueous solution using *Syzygium cumini* leaves: A comparative study of acidic and basic dyes on a single adsorbent. *Koreaz J. Chem. Eng.* **32**, 882–895 (2015).
97. Kannan, C., Buvaneswari, N. & Palvannan, T. Removal of plant poisoning dyes by adsorption on tomato plant root and green carbon from aqueous solution and its recovery. *Desalination* **249**, 1132–1138 (2009).
98. Kulkarni, M. R., Revanth, T., Acharya, A. & Bhat, P. Removal of crystal violet dye from aqueous solution using water hyacinth: equilibrium, kinetics and thermodynamics study. *Resoure-Efficient Technologies* **3**, 71–77 (2017).
99. Wang, X. S. *et al*. Comparison of basic dye crystal violet removal from aqueous solution by low-cost biosorbents. *Separ. Sci. Technol.* **43**, 3712–3731 (2008).
100. Kyzas, G. Z., Lazaridis, N. K. & Mitropoulos, A. C. Removal of dyes from aqueous solutions with untreated coffee residues as potential low-cost adsorbents: equilibrium, reuse and thermodynamic approach. *Chem. Eng. J.* **189–190**, 148–159 (2012).
101. Aniagor, C. O. & Menkiti, M. C. Kinetics and mechanistic description of adsorptive uptake of crystal violet dye by lignified elephant grass complexed isolate. *J. Environ. Chem. Eng.* **6**, 2105–2118 (2018).
102. Shakoor, S. & Nasar, A. Adsorptive decontamination of synthetic wastewater containing crystal violet dye by employing *Terminalia arjuna* sawdust waste. *Groundwater for Sustainable Development* **7**, 30–38 (2018).
103. Doğan, M., Abak, H. & Alkan, M. Adsorption of methylene blue onto hazelnut shell: Kinetics, mechanism and activation parameters. *J. Hazard. Mater.* **164**, 172–181 (2009).
104. Qiu, H. *et al*. Critical review in adsorption kinetic models. *J. Zhejiang Univ. - Sci. A.* **10**, 716–724 (2009).

Acknowledgements

Author Contributions

F.M. conceived and performed the experiments. AN supervised the work. I. and A.M.A. analyzed and interpreted the data and assisted F.M. and A.N in writing the manuscript. All authors discussed the data and agreed to submit the manuscript.

Additional Information

Competing Interests: The authors declare no competing interests.

Publisher's note: Springer Nature remains neutral with regard to jurisdictional claims in published maps and institutional affiliations.